P6.2 AN EVALUATION OF "RKW THEORY" USING A MODEL INTERCOMPARISON

George H. Bryan, Jason C. Knievel,
National Center for Atmospheric Research, Boulder, Colorado

and Matthew D. Parker
University of Nebraska – Lincoln, Lincoln, Nebraska

1. INTRODUCTION

In this paper, we present preliminary results from an intercomparison of idealized squall lines simulated by several numerical models. We focus specifically on the theory put forth by Rotunno et al. (1988), now commonly referred to as RKW Theory. Recently, this theory has been revisited using numerical simulations by Weisman and Rotunno (2004, hereafter referred to as WR04).

The main tenet of RKW theory is that squall line structure is influenced strongly by two effects: the low- to mid-level vertical shear in the environment; and the system's surface-based cold pool. The theory argues for an optimal state wherein these two effects are approximately in balance. In principle, the deepest lifting and the most effective retriggering of cells are obtained when this optimal state is achieved. We evaluate whether our numerical simulations support these conclusions.

2. METHODOLOGY

2.1 Simulation Design

The design of the numerical simulations is generally the same as that used by WR04. Therefore, the resolution, physics schemes, and environmental conditions are constrained by the choices made by WR04. With this new study we seek to answer the very specific question of whether various numerical modeling systems support the conclusions of Rotunno et al. (1988) and WR04 when using the same methodology.

However, one difference between this study and that of WR04 is the domain dimensions, which are 600 km x 80 km x 20 km herein. The slightly deeper domain (20 km as opposed to 17.5 km used by WR04) is necessary to accommodate a Rayleigh damper at the top of the domain instead of an open-radiative condition. The smaller along-line dimension (80 km as opposed to 160 km used by WR04) is used to reduce the cost of the simulations, and is found to be sufficient to address all qualitative and quantitative conclusions.

In all other respects, the simulation details are the same as used by WR04. The squall line is initiated with a 1.5-K line thermal, with small-amplitude perturbations inserted into the line thermal. The horizontal grid spacing is 1 km and the vertical grid spacing is 500 m. The initial thermodynamic environment is the analytic sounding of Weisman and Klemp (1982).

Corresponding author address: George H. Bryan, NCAR/MMM, 3450 Mitchell Lane, Boulder, CO 80301. E-mail: gbryan@ucar.edu

In this study, we investigate only wind profiles with across-line shear in the 0–5 km layer. Linear shear is specified from 0 to 5 km, with a constant wind above 5 km. We refer to the simulations by the amount of wind variation in the 0–5 km layer (ΔU).

2.2 Numerical Models

Results from four numerical models are presented in this study. All are compressible models, using a time-splitting technique to account for the acoustic modes (e.g., Skamarock and Klemp 1992). For three of the models, two different model configurations are used. Thus, there is a total of seven output members considered herein, as summarized in Table 1.

One of the members is the Klemp-Wilhelmson (KW) Model used by WR04. This model uses leapfrog-in-time integration with fourth-order derivatives for horizontal advection and second-order derivatives for vertical advection (Klemp and Wilhelmson 1978; Wilhelmson and Chen 1982). To control numerical noise, a fourth-order artificial diffusion term is used in the horizontal and a second-order vertical diffusion term acting on perturbation fields is used in the vertical.

The second numerical model is the Advanced Regional Prediction System (ARPS; Xue et al. 2000) version 4.5.2. This model also uses leapfrog-in-time integration. For one configuration, referred to as ARPS-A, the model design is similar to the KW design. Fourth-order advection is used in all directions. Fourth-order diffusion is applied in the horizontal only, with the diffusion coefficient being the default value for ARPS 4.5.2, which is roughly one-half of that used by WR04. There is no artificial vertical diffusion term for these simulations. For the second configuration, ARPS-B, the advection of scalars is handled by a flux corrected transport scheme (Zalesak 1979), and the artificial diffusion of scalars is turned off.

The third numerical model is version 2.0.1 of the Weather Research and Forecasting (WRF) Model (Skamarock et al. 2001). Specifically, we use the Eulerian height core of this model, which utilizes a hydrostatic pressure vertical coordinate. This is the only model herein that does not use Cartesian height as the vertical coordinate. This model uses third-order Runge-Kutta time integration (Wicker and Skamarock 2002). The advection formulation is fifth-order in the horizontal and third-order in the vertical. These upwind-biased schemes are implicitly diffusive, so no artificial diffusion term is used. The two WRF Model configurations use different values for C_k, a parameter in the subgrid diffusion scheme that is proportional to the amount of diffusion applied by this scheme (Takemi and Rotunno

Table 1. Summary of the numerical model configurations.

Model	Advection (horiz./vert.)	Special configuration	Diffusion (horiz./vert.)
KW	4^{th} / 2^{nd}		4^{th} / 2^{nd}
ARPS-A	4^{th} / 4^{th}		4^{th} / none
ARPS-B	4^{th} / 4^{th} (except for scalars)	Scalar adv. is FCT / FCT	4^{th} / none (*u, v, w* only)
WRF-A	5^{th} / 3^{rd}	C_k = 0.10	Implicit, flow dependent
WRF-B	5^{th} / 3^{rd}	C_k = 0.15	Implicit, flow dependent
BF-A	5^{th} / 5^{th}		Implicit, flow dependent
BF-B	5^{th} / 5^{th} (except for scalars)	Scalar adv. is WENO / WENO	Implicit, flow dependent

2003). One configuration, WRF-A, uses a typical value, C_k = 0.10. The second configuration, WRF-B, uses C_k = 0.15.

The fourth numerical model is version 1.8 of the Bryan-Fritsch (BF) cloud model (Bryan and Fritsch 2002). This model uses the Runge-Kutta time integration technique, and an equation set that has improved conservation of total mass and total energy. For one configuration, BF-A, the advection scheme is fifth-order in all directions, with no artificial diffusion. For the other configuration, BF-B, the advection of scalars uses the Weighted Essentially Non-Oscillatory (WENO) scheme of Shu (2001).

In summary, there are six simulation members that use relatively newly developed numerical models — ARPS, WRF, and BF. Three of the members are configured with comparatively low diffusion, and are denoted with "-A." The second set of three members, denoted with "-B," have either increased diffusion, or use nonoscillatory advection schemes, which are typically more diffusive than default oscillatory schemes.

3. RKW THEORY

3.1 System Structure

WR04 showed that a broad range of system structure can be produced by numerical models through the increase of low- to mid-level shear. With weak 0–5 km shear, the simulated systems are upshear-tilted and contain mainly weak, scattered updrafts (Figs. 12a–b and 13a–b of WR04). With moderate 0–5 km shear, simulated systems are more upright, and updrafts are more continuous along the line (Figs. 12c and 13c of WR04). With even stronger 0–5 km shear, the systems are downshear-tilted, with strong, isolated cells having supercellular characteristics (Figs. 12d and 13d of WR04).

These qualitative conclusions also hold for all six members using the newer models. That is, the trend from upshear-tilted to downshear-tilted systems with increasing 0–5 km shear occurs in all simulations. Line-averaged vertical cross sections reveal similar structures overall, with mostly minor differences between models. An example for ΔU = 10 m s^{-1} is shown in Fig. 1. All models produce structures that are broadly similar, with the cold pool being deepest within 20–30 km of the surface gust front, and a cloud pattern that extends mostly upshear of the gust front.

One of the more notable differences is the tendency for the more diffusive "B" simulations to have weaker cold pools and less developed convective systems. For example, the ARPS-B and BF-B simulations have a considerably narrower upper-tropospheric cloud. This difference can be directly attributed to the enhanced diffusion in these simulations, which weakens the updrafts, leading to less condensation and less total evaporation.

For ΔU = 10 m s^{-1}, the WRF-B results are not much different than the WRF-A results (Figs. 1c and 1d). However, this result does not hold for all shears. For example, for ΔU = 0 m s^{-1}, increasing C_k from 0.10 to 0.15 practically eliminates all cells in the convective region (Figs. 2c and 2d).

Another difference between models is the tendency for the KW model results to have the deepest and strongest cold pools. For the ΔU = 10 m s^{-1} case, the analogous figure from WR04 (Fig. 12b) has the –0.01 m s^{-2} buoyancy value at a height of 2 km at all locations west of the cloud boundary. In contrast, this value is below 1.5 km, and typically below even 1.25 km, for all simulations in Fig. 1. This tendency for the KW Model to have the strongest cold pools is the most salient result from this intercomparison. An explanation for this result is offered in section 4.

We also find that the weakly diffusive "A" simulations are often characterized by a curiously artificial updraft pattern (Fig. 2). That is, the cells are often poorly resolved, and sometimes have a strangely repeating pattern, especially when the low-level shear is weak. This is probably the same pattern noted by Takemi and Rotunno (2003). The cause of this curious pattern, including an explanation for why it only occurs with weak low-level shear, is explored further by Bryan (2004, manuscript submitted to *Mon. Wea. Rev.*).

With the KW Model, the convective cells at 3 km are larger and do not show evidence of this artificial organization (Fig. 13b of WR04). We attribute this difference in cellular structure to stronger artificial diffusion in the KW Model simulations.

Despite these differences in details, for all model configurations the trend in system structure with increasing shear is broadly similar to that found by WR04. That is, low-level and mid-level updraft intensity increases and cells become larger as environmental shear increases.

In summary, there are some differences in system structure between the models, but the overall qualitative structures are very similar. The trend from weak,

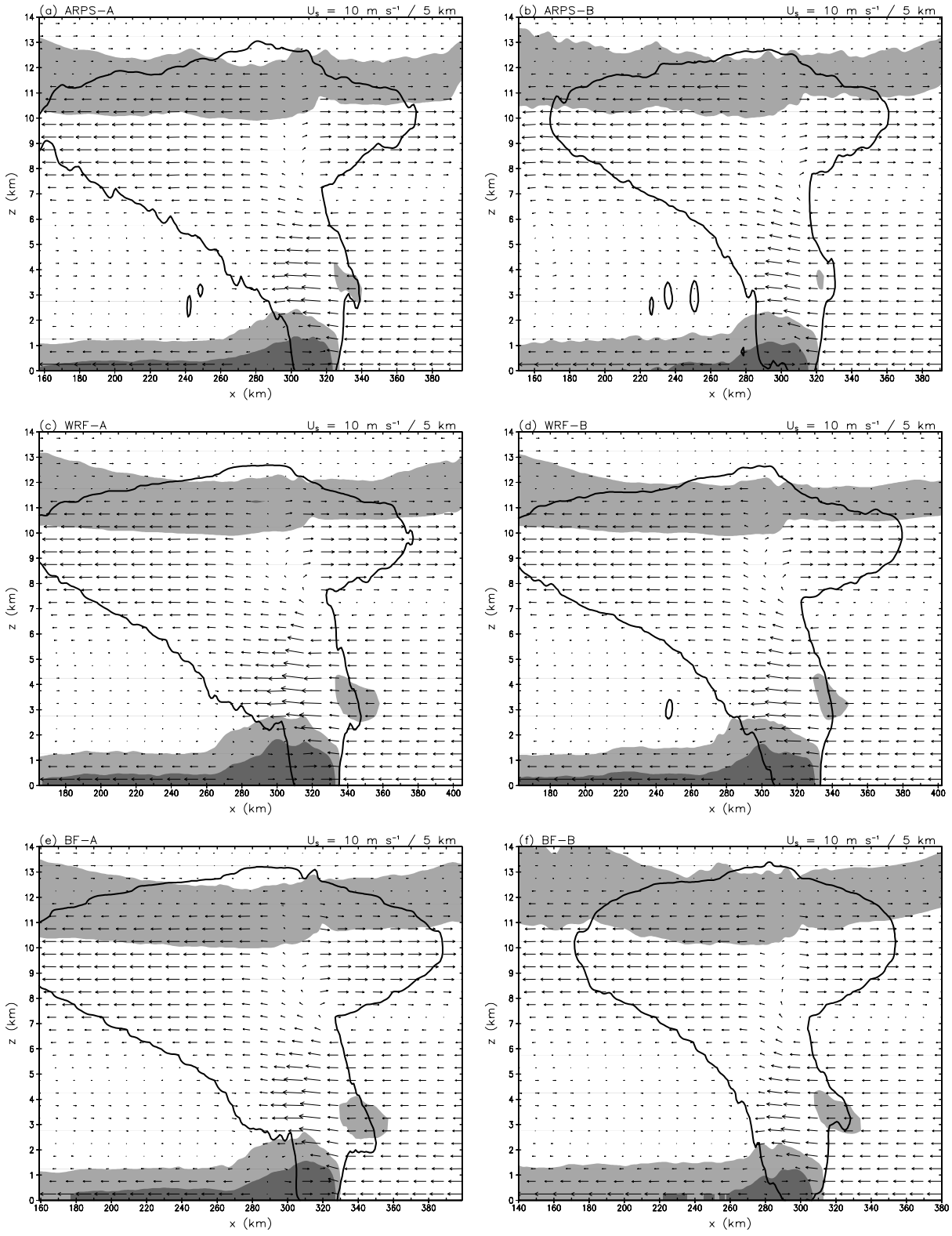

Fig. 1. Line-averaged cross sections at t = 4 h for ΔU = 10 m s^{-1} and (a) ARPS-A, (b) ARPS-B, (c) WRF-A, (d) WRF-B, (e) BF-A, and (f) BF-B. System-relative flow vectors are included every 10 km horizontally and every 500 m vertically, with a vector length of 10 km representing a vector magnitude of 15 m s^{-1}. The 1×10^{-2} g kg^{-1} cloudwater contour indicates the cloud boundary. Buoyancy is shaded, with light grey representing < –0.01 and dark grey representing < –0.1 m s^{-2}.

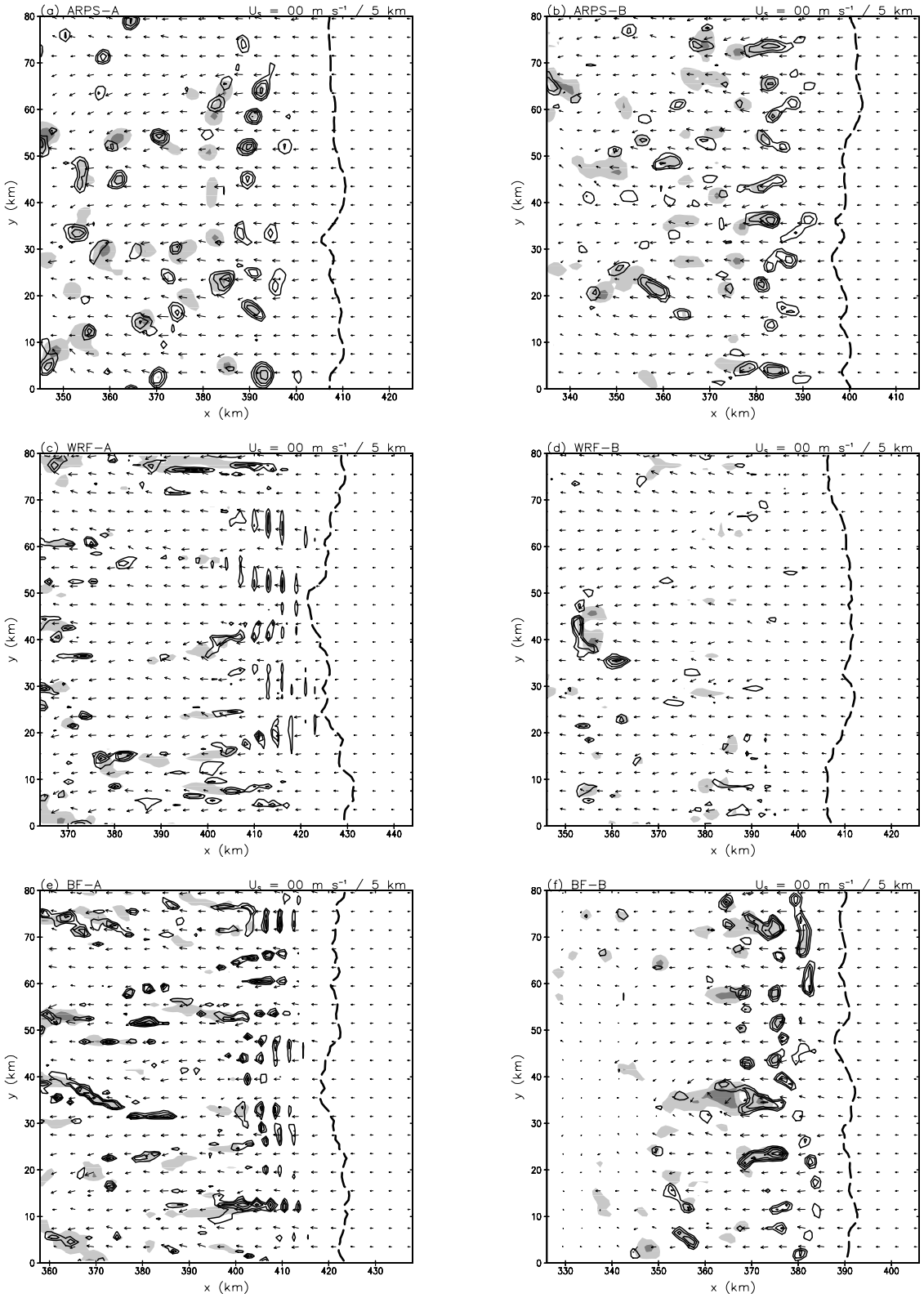

Fig. 2. Horizontal cross sections at z = 3 km and t = 4 h for ΔU = 0 m s^{-1} and (a) ARPS-A, (b) ARPS-B, (c) WRF-A, (d) WRF-B, (e) BF-A, and (f) BF-B. Positive vertical velocity is contoured every 2 m s^{-1}. Rainwater mixing ratio is shaded, with light grey representing > 1 and dark grey representing > 4 g kg^{-1}. Line-relative flow vectors are included every 4 km, with a vector length of 4 km indicating a vector magnitude of 20 m s^{-1}. The thick dashed contour is the surface gust front.

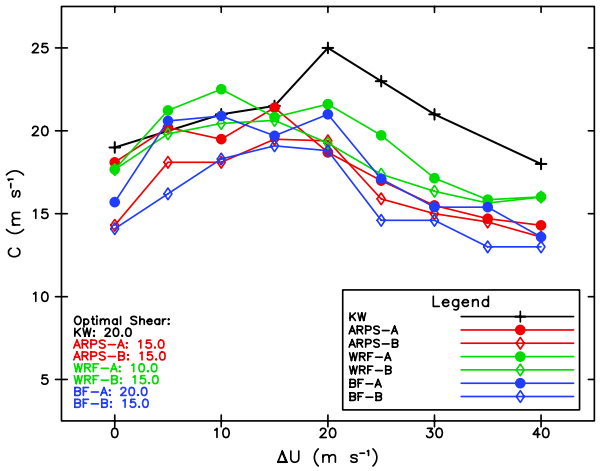

Fig. 3. Average C (m s^{-1}) from 3-6 h versus ΔU for the seven model configurations. The data labeled "Optimal Shear" in the lower-left corner indicate the value of ΔU for which C is a maximum.

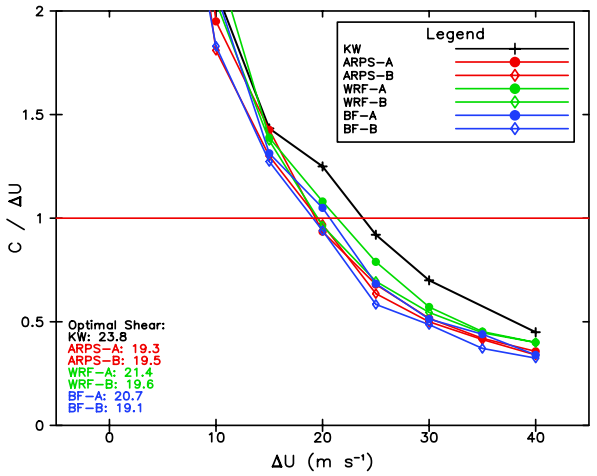

Fig. 4. Average C / ΔU from 3-6 h versus ΔU. The horizontal red line is where C / ΔU = 1. The data labeled "Optimal Shear" in the lower-left corner indicate the estimated value of ΔU for which C / ΔU = 1.

upshear-titled systems in weak shear to strong, downshear-tilted systems in strong shear is clearly captured in all simulations. This specific aspect of RKW Theory — that low- to mid-level shear alone can produce a broad range of system structure, all else being equal — is confirmed by all numerical models used herein.

3.2 An Optimal State

A more controversial aspect of RKW Theory is the existence of an optimal state, wherein the cold pool circulation roughly balances the circulation associated with the environmental low-level shear. When this balance occurs, the lifting at the leading edge of the system should be the strongest and deepest. The effect of this balance on other system properties, such as overall system intensity, is less clear.

WR04 evaluated this optimal state via C, a measure of cold pool depth and intensity, and ΔU, a measure of shear in low- to mid-levels. Rotunno et al. (1988) and WR04 argued that the optimal state occurs when the ratio C / ΔU is approximately 1.

Mathematically, C is represented by

$$C^2 = 2\int_0^H (-B)dz\,, \qquad (1)$$

wherein H is the cold pool depth and B is buoyancy (WR04). We calculate C from the model output in the same manner as WR04, except we use only hourly output from t = 3 to 6 h.

Rotunno et al. (1988) first proposed the 0–2.5 km layer as the relevant depth for calculations of ΔU. However, based on a more extensive set of simulations, WR04 now recommend 0–5 km. We follow the suggestion of WR04 and define ΔU as the wind change in the lowest 5 km.

Calculations of C confirm the qualitative conclusion that the KW Model usually produces the deepest, strongest cold pools (Fig. 3). The only exception is for weak shears, for which results from the KW Model are similar to the "A" model configurations.

All models produce a peak C value when ΔU is between 10 and 20 m s^{-1}, with the average optimal shear value being 15.7 m s^{-1}. Thus, the notion of an optimal shear for which C is maximized is supported by all models.

We also present C / ΔU plotted as a function of ΔU (Fig. 4). In this figure, the shear value where these curves cross C / ΔU = 1 is indicated at the bottom-left corner of the figure. This analysis shows that the KW Model produces the optimal state for a larger shear, $\Delta U \approx 24$ m s^{-1}, than the other six models, which have an average optimal shear of $\Delta U \approx 20$ m s^{-1}.

To determine whether this optimal condition has any relevance to system properties, we present the total rainfall as a function of shear in Fig. 5. Once again, the KW Model is an outlier for the high shears; it produces more rainfall than any other model for ΔU = 20 to 40 m s^{-1}. Furthermore, the rainfall is maximized with the KW Model at a considerably higher ΔU of 30 m s^{-1}, as opposed to an average ΔU of 19 m s^{-1} for the other models.

Some models tend to have a pronounced increase in maximum surface winds when ΔU increases from 35 to 40 m s^{-1}. In this high shear environment, the simulated cells are supercellular, which is a structure to which RKW Theory does not apply. For the environment between ΔU = 0 and 30 m s^{-1}, there is again evidence for an optimal shear; for the ARPS, WRF, and BF Model runs, the average shear for which surface winds are maximized is ΔU = 20 m s^{-1}.

The overall conclusion from this analysis is that the

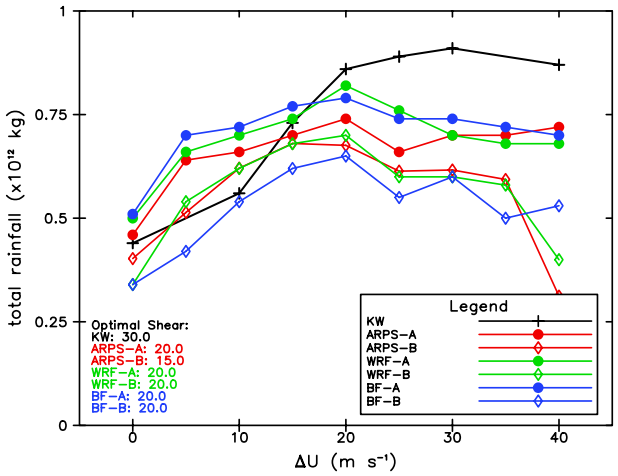

Fig. 5. Total rainfall ($\times 10^{12}$ kg) from 1–6 h versus ΔU. Total rainfall from the ARPS, WRF, and BF Models is multiplied by 2 to account for the smaller domain size compared to the KW Model simulations. The data labeled "Optimal Shear" indicate the value of ΔU for which total rainfall is a maximum.

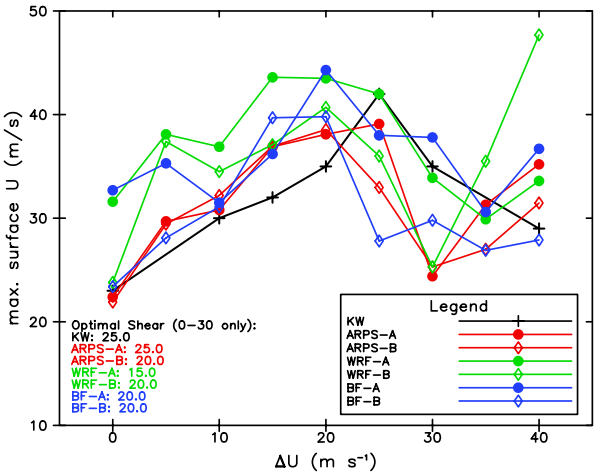

Fig. 6. Maximum *u* (m s^{-1}) at the lowest model level versus ΔU from 3–6 h. The data labeled "Optimal Shear" indicate the value of ΔU (between 0 and 30 m s^{-1} only) for which *u* at the lowest model level is a maximum.

newer models — the ARPS, WRF, and BF Models — provide more support for the existence of an optimal state than does the KW Model. The ratio *C* / ΔU is approximately 1 when ΔU is 20 m s^{-1}. This is also the same shear when, on average, total rainfall is maximized and surface winds are strongest.

4. MODEL COLD POOL BIAS

The second main goal of this study is to determine whether there are any notable biases in any of the models. For idealized simulations such as these, there is no absolute "truth" solution to compare against. However, in comparing numerical simulations from the four models, we have identified some notable differences and, in some cases, have uncovered errors in model code. A similar conclusion on the utility of model intercomparisons was drawn by Redelsperger et al. (2000).

The only major model bias we find is the tendency for the KW Model to produce more intense surface-based cold pools, especially for higher shears (e.g., Fig. 3). An investigation into this difference leads us to conclude that the artificial vertical diffusion scheme in the KW Model is responsible. The use of artificial vertical diffusion alone is not the cause of these anomalously strong cold pools; rather, a difference in how the diffusion is applied near the boundaries is ultimately responsible.

In the KW Model, artificial vertical diffusion is not applied at the grid points closest to the bottom and top boundaries. If vertical diffusion is written in flux form, this is equivalent to making equal the flux at the boundaries and the flux at the nearest grid point inside the domain. Thus, the KW Model can have a non-zero flux at the top and bottom boundaries. All other models have a zero-flux boundary condition at the top and bottom, including the artificial vertical diffusion scheme in the ARPS Model.

Throughout most of the domain, this boundary flux is approximately zero, because the diffusion acts on perturbations. Specifically, the effective boundary flux at the surface is

$$F_{sfc} = -K \left. \frac{\partial \alpha'}{\partial z} \right|_{k=1}, \qquad (2)$$

wherein *K* is the diffusion coefficient, α is the variable being diffused, and the prime indicates the deviation from the model's base state, which in these simulations is the model initial condition. In the environment ahead of and far behind the squall line, the environment near the surface remains approximately the same as the initial state; thus, $\alpha' \cong 0$, and $F_{sfc} \cong 0$. However, in the squall line's cold pool, the potential temperature perturbation (θ') is negative at the lowest model level and decreases in magnitude with height. Thus, $\partial\theta'/\partial z > 0$, $F_{sfc} < 0$ for θ', and the result is a net artificial source of cooling at the lowest model level. For water vapor, the perturbation is usually negative in the cold pool at the surface and decreases (becomes more negative) with height, resulting in a net artificial source of moistening at the lower boundary. The combination of cooling and moistening at the surface results in approximately no change in equivalent potential temperature. The same boundary condition acts on horizontal winds, and tends to artificially increase surface winds in the cold pool.

The same conclusion concerning the vertical diffusion scheme was reached by Richardson (1999) in a comparison between the KW and ARPS Models. We believe a zero flux boundary condition is the better choice because the alternative configuration provides an artificial source of mass through the lower boundary in cold pools.

5. CONCLUSIONS

These preliminary results of a model intercomparison have produced some interesting results. First, from a technical perspective, we have found this project to be very useful for identifying differences between the models that, in some cases, have led us to uncover coding errors. We recommend that intercomparison studies should explore a broad physical parameter space, such as environmental shear. In some cases, the models only revealed their biases when results as a function of shear were presented. For example, the bias in the KW Model is not apparent for low shears, but becomes obvious when a broad range of shears are simulated.

A second major result is support for RKW Theory. In terms of system structure, all models produce the same qualitative conclusion for changes in shear, with all else being held constant. That is, the squall lines had weaker cells and were tilted upshear in weak 0–5 km shear, and had larger, stronger cells and were tilted downshear with strong 0–5 km shear. Analysis of cold pool structure suggests an optimal state when $\Delta U = 20$ m s^{-1} for all models except the KW Model. Furthermore, total rainfall and maximum surface winds were maximized at the same value of $\Delta U = 20$ m s^{-1} for all models except the KW Model. This study does not address all concerns expressed in the literature about RKW Theory. Future studies could explore the use of ice microphysics and higher resolution, for example.

Finally, we diagnosed the reason why the KW Model produces the deepest and strongest cold pools. The vertical diffusion formulation near the lower boundary acts as an artificial source of cooling and moistening in the simulated cold pool. Other model differences, such as noisy updraft patterns and differing cloud water distribution, had no perceptible impact on the theory being analyzed here.

Acknowledgments

We thank Morris Weisman for inspiring this study. The MMM Division at NCAR provides the version of the WRF Model used here, and the Center for Analysis and Prediction of Storms provides the ARPS Model. NCAR's Advanced Study Program supported G. Bryan. NCAR is supported by the National Science Foundation.

REFERENCES

Bryan, G. H., 2004: Spurious convective organization in simulated squall lines owing to moist absolutely unstable layers. *Mon. Wea. Rev.,* submitted.

Bryan, G. H., and J. M. Fritsch, 2002: A benchmark simulation for moist nonhydrostatic numerical models. *Mon. Wea. Rev.,* **130**, 2917–2928.

Klemp, J. B., and R. B. Wilhelmson, 1978: The simulation of three-dimensional convective storm dynamics. *J. Atmos. Sci.,* **35,** 1070–1096.

Redelsperger, J. L., and coauthors, 2000: A GCSS model intercomparison for a tropical squall line observed during TOGA-COARE. I: Cloud-resolving models. *Quart. J. Roy. Meteor. Soc.,* **126,** 823–863.

Richardson, Y., 1999: The influence of horizontal variations in vertical shear and low-level moisture on numerically simulated convective storms. Ph. D. dissertation, University of Oklahoma. [Available from School of Meteorology, university of Oklahoma, 100 E. Boyd, Norman, OK 73019.]

Rotunno, R., J. B. Klemp, and M. L. Weisman, 1988: A theory for strong, long-lived squall lines. *J. Atmos. Sci.,* **45**, 463–485.

Shu, C.-W., 2001: High order finite difference and finite volume WENO schemes and discontinuous Galerkin methods for CFD. ICASE Report No. 2001-11, 16 pp. [Available from NASA Langley Research Center, Hampton, VA, 23681-2199.]

Skamarock, W. C., and J. B. Klemp, 1992: The stability of time-split numerical methods for the hydrostatic and nonhydrostatic elastic equations. *Mon. Wea. Rev.,* **120,** 2109–2127.

Skamarock, W. C., J. B. Klemp, and J. Dudhia, 2001: Prototypes for the WRF (Weather Research and Forecasting) model. Preprints, *14th Conference on Numerical Weather Prediction,* Fort Lauderdale, FL, Amer. Meteor. Soc. J11–J15.

Takemi, T., and R. Rotunno, 2003: The effects of subgrid model mixing and numerical filtering in simulations of mesoscale cloud systems. *Mon. Wea. Rev.,* **131,** 2085–2101.

Weisman, M. L., and J. B. Klemp, 1982: The dependence of numerically simulated convective storms on vertical wind shear and buoyancy. *Mon. Wea. Rev.,* **110,** 504–520.

Weisman, M. L., and R. Rotunno, 2004: "A theory for strong long-lived squall lines" revisited. *J. Atmos. Sci.,* **61,** 361–382.

Wicker, L. J., and W. C. Skamarock, 2002: Time splitting methods for elastic models using forward time schemes. *Mon. Wea. Rev*., **130**, 2088–2097.

Wilhelmson, R. B., and C.-S. Chen, 1982: A simulation of the development of successive cells along a cold outflow boundary. *J. Atmos. Sci.,* **39,** 1466–1483.

Xue, M., K. K. Droegemeier, and V. Wong, 2000: The Advanced Regional Prediction System (ARPS) – A multiscale nonhydrostatic atmospheric simulation and prediction model. Part I: Model dynamics and verification. *Meteor. Atmos. Phys.,* **75,** 161–193.

Zalesak, S. T., 1979: Fully multidimensional flux-corrected transport algorithms for fluids. *J. Comput. Phys.,* **31,** 335–362.